Ammonia synthesis on graphitic-nanofilament supported Ru catalysts

Zhonglai Li, Changhai Liang, Zhaochi Feng, Pinliang Ying, Dezheng Wang[1], Can Li[*]

State Key Laboratory of Catalysis, Dalian Institute of Chemical Physics, Chinese Academy of Sciences, Dalian 116023, China

Abstract

Graphitic-nanofilaments (GNFs) supported ruthenium catalysts were prepared and characterized by N_2 physisorption, X-ray diffraction (XRD), transmission electron microscope (TEM) and temperature programmed reduction-mass spectroscopy (TPR-MS) and used for ammonia synthesis in a fixed bed microreactor. The TEMs of the Ru/GNFs and Ru-Ba/GNFs catalysts indicate that the Ru particles are in the range of 2–4 nm, which is the optimum size of Ru particles for the maximum number of B5 type sites. The activity of Ru-Ba/GNFs catalysts is higher than that of Ru-Ba/AC by about 25%. The methanation reaction on the Ru/GNFs catalyst is remarkably inhibited compared with a Ru/AC catalyst. High graphitization of GNFs is likely to be the reason for the high resistance to the methanation reaction. The power rate law for ammonia synthesis on Ru-Ba/GNFs catalysts can be expressed by $r = K P_{NH_3}^{-0.4} P_{N_2}^{0.8} P_{H_2}^{-0.7}$, indicating that H_2 is an inhibitor for N_2 activation on the catalyst. Catalysts with the promoters Ba, K and Cs show large differences in activity for ammonia synthesis. The catalyst promoted with Ba (Ba/Ru = 0.2 molar ratio) was found to be the most active, whereas that with a K promoter was the least active.
© 2003 Elsevier B.V. All rights reserved.

Keywords: Ammonia synthesis; Graphitic-nanofilaments; Ru; Promoter; Kinetics

1. Introduction

The synthesis of ammonia from nitrogen and hydrogen is one of the most important catalytic processes. Conventional multi-promoted iron-based catalysts have been used for ammonia synthesis since 1913. High temperatures and high pressures are required for ammonia synthesis on conventional Fe-based catalysts. Hence, new catalysts operating under mild conditions are desired in order to further decrease energy costs. Ru supported on active carbon promoted by potassium was found to be more active than iron catalysts for ammonia synthesis in 1971 [1]. Low temperatures and pressures are both important advantages of the Ru/AC catalysts over conventional multi-component iron-based catalysts. A plant was constructed that commercialized carbon-supported Ru catalysts promoted by alkali and alkali-earth metals in the 1990s by a group comprised of Kellog, Engelhard and British Petroleum. Since then, Ru-based catalysts have

attracted a great deal of attention from academic and industrial circles, and have the potential to replace conventional iron-based catalysts for ammonia synthesis. Many studies have focused on activated carbon (AC) supported Ru catalysts. However, extensive studies show that the deactivation of the catalyst is a serious problem under the reaction conditions when Ru was deposited onto the surface of the activated carbon. There are three considerations on this problem in the literature, i.e. metal sintering, loss of the active component and methanation of the support, of which the last becomes obvious when the catalyst has been operated under working conditions for a long time [2–6]. Therefore, a more stable support is required, and this has led to a search for an alternative to active carbon. Recently, a number of studies have shown that graphitzed activated carbon, MgO and BN supported Ru have high catalytic activities and long-term stability for ammonia synthesis [4–13].

Aika and co-workers [4], Forni et al. [6] and Kowalczyk et al. [9] found that the catalyst lifetime was remarkably prolonged when the activated carbon was treated at high temperatures. These results reveal that graphitized carbon is feasible as a catalyst support for ammonia synthesis. In 1991, a novel carbon material named carbon nanotubes (CNTs) was discovered [14], which is produced by arc-discharge at high temperatures. Later, a similar material

* Corresponding author. Tel.: +86-411-4379070;
fax: +86-411-4694447.
E-mail address: canli@dicp.ac.cn (C. Li).
URL: http://www.canli.dicp.ac.cn.
[1] Department of Chemical Engineering, Tsinghua University, Beijing 100084, China.

named graphitic-nanofilaments (GNFs) were obtained by the dissociation of methane on Ni, Co or Fe catalysts at high temperatures [15]. These materials have attracted a great deal of interest in many fields due to their peculiar one-dimensional structure consisting of rolled up graphene sheets with a unique electronic structure. It was shown that the graphitic-nanofilaments possess metallic or semiconducting properties when the carbon is intercalated with metal particles [16]. Compared to activated carbon, GNFs have a "clean" surface and no impurity components in the bulk due to their special formation process. GNFs can be an ideal support because they are free of the harmful influences of N, S and Cl impurities on the activation of reactants [5,17]. Recently, the catalytic performance of K-Ru supported on multi-walled carbon nanotubes was investigated and high activity for ammonia synthesis was obtained [18]. In our previous experiments [19], it was found that barium promoted Ru/GNFs catalysts exhibited remarkably high activity for ammonia synthesis. In this paper, Ru supported on GNFs catalysts were prepared and characterized for ammonia synthesis. The effects of promoters, GNFs types and size of Ru particles, resistance to methanation and the kinetics of ammonia synthesis on Ru-Ba/GNFs were investigated in detail.

2. Experimental

2.1. Catalyst preparation

Graphitic-nanofilaments were synthesized by the catalytic decomposition of methane on a Co catalyst and is denoted as GNFs-A, and on Ni catalyst which is denoted as GNFs-B, respectively [20]. The raw samples were treated with 6 M HNO_3 at room temperature to eliminate residual metal (Co or Ni) and support. After washing with distilled water, the sample was refluxed with 6 M HNO_3 for 4 h in an oil bath at 140 °C to remove amorphous carbon and increase surface oxygen functional groups, which are favorable for metal deposition and dispersion.

GNFs were impregnated with an acetone solution of $RuCl_3 \cdot 3H_2O$. After drying in air at 100 °C overnight, the samples with different Ru content were reduced in an H_2 flow at 450 °C for 8 h, followed by cooling to room temperature in hydrogen and then passivation. Subsequently, the Ru/GNFs sample was impregnated with an aqueous solution of $Ba(NO_3)_2$, KOH, $CsNO_3$, then reduced with an H_2 flow by the same procedure as above.

2.2. Catalytic activity test

Ammonia synthesis was performed in a stainless steel fixed bed reactor system [8]. For the steady state measurement of catalytic activity, the reactor was filled with the Ru/GNFs catalyst diluted with 20–60 meshes quartz particles as the catalyst bed. It was previously determined that quartz particles are not active for ammonia synthesis. Reac-

tion orders of NH_3, N_2 and H_2 were determined by changing the concentration of one reactant while keeping the others fixed [21]. The experiments were carried out in a temperature range from 325 to 450 °C, using N_2 and H_2 molar ratios from 1:3 to 3:1. The reaction order for ammonia was determined by varying the mixture gas flow from 30 to 90 ml min^{-1} (STP). The activation energy of reaction was measured by changing the temperature between 325 and 400 °C.

2.3. Catalyst characterization

BET surface area of the graphitic-nanofilaments was measured by N_2 physisorption at –196 °C using a Micromeritcs ASAP 2000 instrument. X-ray diffraction (XRD) patterns were obtained on a Rigaku Rotaflex R-200B diffractometer with Cu Kα radiation (λ = 1.5418 Å). A transmission electron microscope (TEM, Jeol JEM-2000EX) was used to confirm the shape of the graphitic-nanofilaments and the morphology of the supported Ru catalysts. The graphitic-nanofilaments and supported Ru catalysts were suspended in an ethanol solvent. After ultrasonic treatment, a drop of the suspension was placed onto a microgrid covered with a carbon film.

Methanation of the support was characterized using H_2-temperature programmed reduction-mass spectroscopy (TPR-MS). Hundred milligrams of catalyst was first treated with H_2 at 30 ml min^{-1} (STP) for 1 h at 100 °C. The temperature was then raised at a heating rate of 10 °C min^{-1} from 100 to 700 °C in the presence of H_2. The m/e signals were analyzed by a quadrupole mass spectrometer (Balzers, QMS 200).

3. Results and discussion

The X-ray diffraction patterns of GNFs, activated carbon, and supported Ru catalysts are shown in Fig. 1. It can be
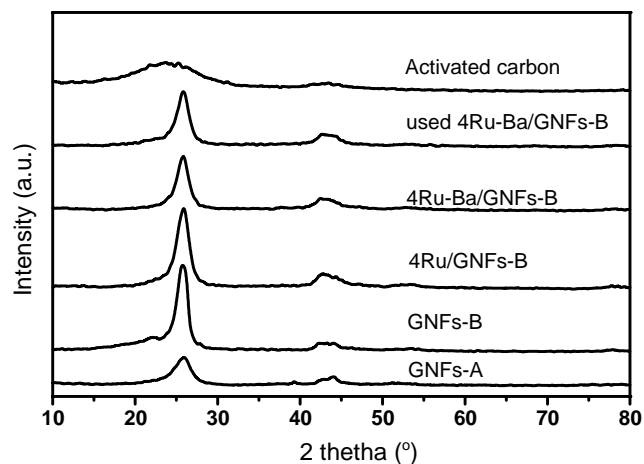

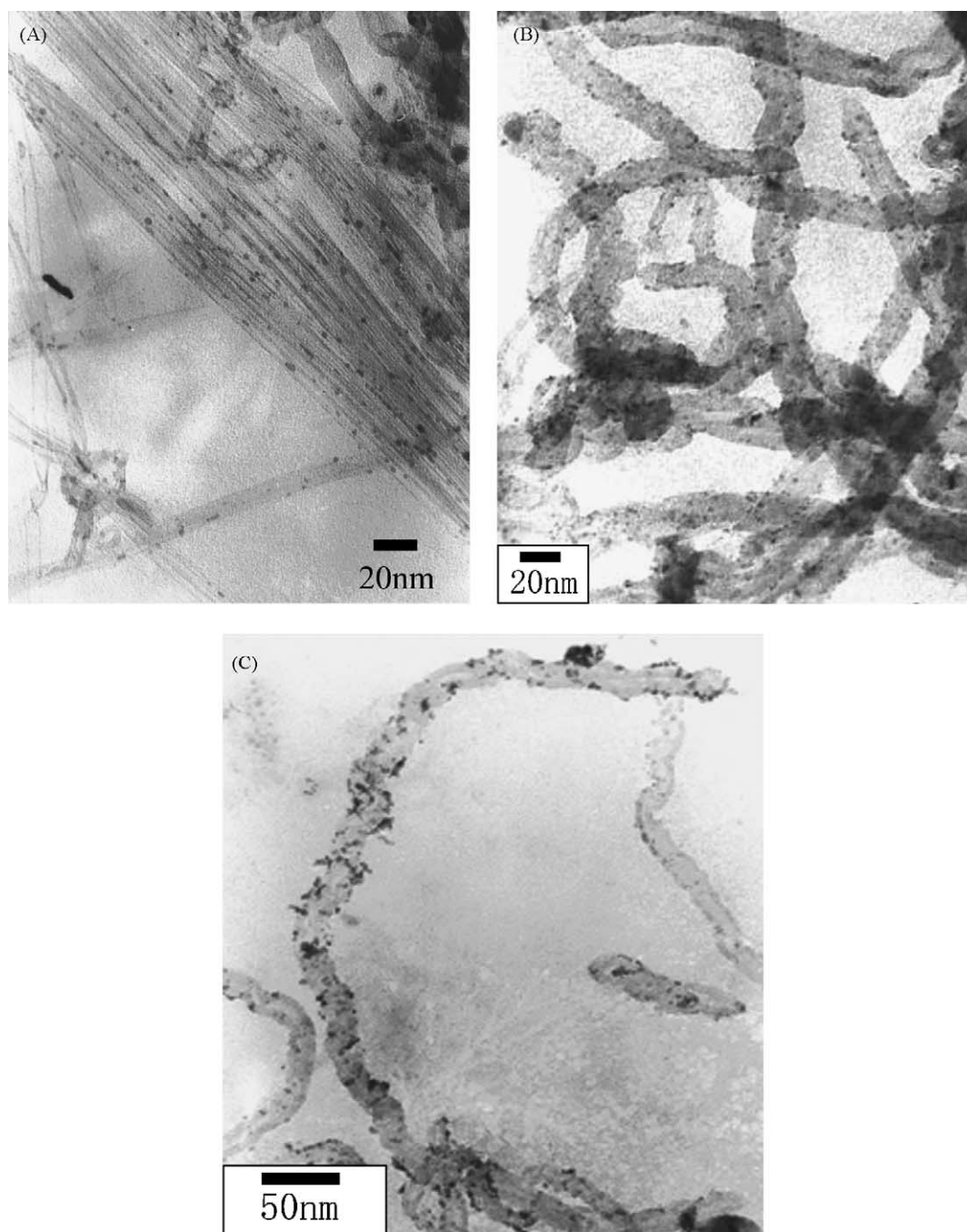Fig. 1. XRD patterns of the GNFs, activated carbon and supported catalysts.

Fig. 2. TEM micrographs of the catalysts. (A) 4 wt.% Ru/GNFs-A, (B) 4 wt.% Ru/GNFs-B, and (C) 8 wt.% Ru/GNFs-B.

seen that the XRD pattern of the graphitic-nanofilaments is remarkably similar to the XRD pattern of graphite, while the XRD pattern of activated carbon indicates an amorphous structure. For the GNFs samples, four peaks for (0 0 2), (0 0 4), (1 0 0) and (1 1 0) are observed. A quite symmetrical and sharp (0 0 2) peak emerges at 26° and a broadened peak (1 0 0) at about 42°. The average interlayer spacing is 0.34 nm according to (0 0 2) crystalline face [22,23]. Some papers have reported that this layered structure of carbon is favorable for the transfer of electrons and a close interaction between the metal and support by intercalation [24,25].

Recently, Jacobsen reported a novel BN material as the catalyst support for ammonia synthesis [13]. It was suggested that BN also possesses a layered structure like graphite, although the relationship between the layered structure and the improved catalytic activity in ammonia synthesis is unclear. For the supported Ru catalysts, no diffraction peak due to metal Ru was detected, indicating that metal Ru is well-dispersed on GNFs.

The hollow concentric cylinders of GNFs were observed by TEM, shown in Fig. 2A and 2B. The outer diameters of GNFs-A and GNFs-B are between 5 and 20, and 20

Table 1
Element analysis and calculated nitrogen BET surface area of GNFs and AC

Support	Surface area (m^2/g)	Density (g/ml)	Element analysis (wt.%)						
			C	H	O	N	Cl	S	Ash
GNFs-A	278	0.27	99.02	0.01	0.97	–	–	–	–
GNFs-B	140	0.30	98.76	0.02	1.22	–	–	–	–
AC	1290	0.50	91.09	0.87	7.75	0.04	0.10	0.15	3.0

and 40 nm, respectively, while the inner diameter ranges from 3 to 10 nm and the length ranges from 60 to 200 μm. Their morphology and surface areas are distinct, as shown in Table 1. The GNFs-A sample contains a small amount of bent tubes and a large amount of straight tubes which are single-walled. GNFs-B samples are all bent nanofilaments. The differences in the GNFs diameter in the TEM images may be attributed to different reaction conditions for methane pyrolysis and used the catalysts. Metal particles of 4 wt.% Ru/GNFs are mainly deposited on the outer surface of the nanofilaments. The TEM micrograph also reveals that the size of the metal particles ranges from 2 to 4 nm on GNFs-A and GNFs-B. The particle size ranges from 4 to 8 nm when the metal loading on GNFs-B is about 8 wt.%, as shown in Fig. 2C. Congregation of the metal particles can be observed and the shape of the metal particles are not spherical when compared to that of 4 wt.% Ru/GNFs-B. It is suggested that both the size and morphology of the Ru crystals are influenced by the interaction between the metal and the support. The sintering of smaller crystals of about 1.0 nm results in larger metal particles. Graphite nanofibers supported Ni were used as hydrogenation catalysts for alkenes and dienes at moderate temperatures by Park and Baker. They also suggested that the crystallographic faces of the metal particles is associated with the type of nanofilament structure used as the supporting medium [26]. Compared with the two types of GNFs supported Ru catalysts, it is interesting to find that straight single-walled nanofilament supported Ru did not show superior activity for ammonia synthesis over bent nanofilament supported Ru (4 wt.% Ru/GNFs-B) although the transfer of electrons on straight tube is believed to be better than the others (Table 2). However, the ammonia synthesis activity of the Ru-based catalysts is much higher than that of Fe-based catalysts at the same reaction conditions.

A comparison of the TPR-MS profiles of $RuCl_3$/GNFs-B and $RuCl_3$/AC is shown in Fig. 3. The intensity signals

of CH_4 evolved from $RuCl_3$/GNFs-B and $RuCl_3$/AC during the reduction process are recorded as a function of the temperature. It is found that above 550 °C the methanation peak of GNFs significantly increases, which is attributed to the reaction of the graphitic-nanofilaments catalyzed by Ru metal on the surface. The initial temperature of methanation on $RuCl_3$/AC is about 500 °C under the same reaction condition. Initial methanation temperatures of $RuCl_3$/GNFs-B and $RuCl_3$/AC indicate that GNFs as a catalyst support is more resistant to the methanation reaction than activated carbon. However, the methanation reaction of GNFs could not be avoided although the initial temperature of the methanation reaction on the GNFs with deep graphitization is higher by about 50 °C than that on activated carbon. Aika and co-workers [4] investigated the methanation reaction of $RuCl_x$/AC catalysts and suggested that activated carbon with deep graphitization can suppress the methanation reaction. The effect of carbon pretreatment on activity in ammonia synthesis was reported by Forni et al. [6], who found that high catalytic activity might come from the graphitization of carbon with the simultaneous removal of impurities at high temperatures under an inert atmosphere.

Fig. 4 shows the catalytic activity for ammonia synthesis on Ru/GNFs-B catalysts with different promoter/Ru atomic ratios under a pressure of 3.0 MPa at 400 °C in a 3:1 mixture of H_2 and N_2. In these experiments, Ru/GNFs-B promoterd by Ba (Ba/Ru = 0.2 atomic ratio) is the most active for ammonia synthesis among the three kinds of promoters tested probably due to the different roles of the promoters [10]. Its activity is four and two times higher than that of Ru/GNFs-B
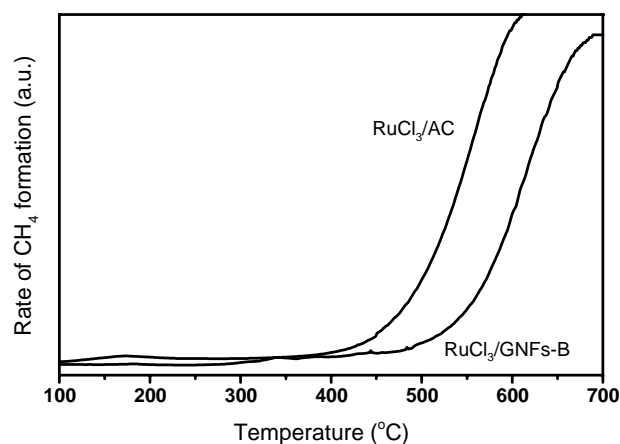
Table 2
Catalyst activity and average size of Ru dispersed on GNFs and AC

Catalyst	Particle size (nm)	Rate of NH_3 synthesis (mmol g^{-1} h^{-1})
Ru/GNFs-A	2.9	18.4
Ru/GNFs-B	2.9	19.1
Ru/AC	2.7	15.0
Fe-based	–	1.2

Note: The reaction was conducted at 673 K and 3.0 MPa using a mixture of $H_2/N_2 = 3$ at a flow of 50 ml min^{-1} (STP). All catalysts were 4 wt.% Ru loading; Ba/Ru molar ratio was 0.2 for Ru/GNFs and 1 for Ru/AC.

Fig. 3. TPH profiles from $RuCl_3$/GNFs-B and $RuCl_3$/AC using a H_2 flow of 30 ml min^{-1}.
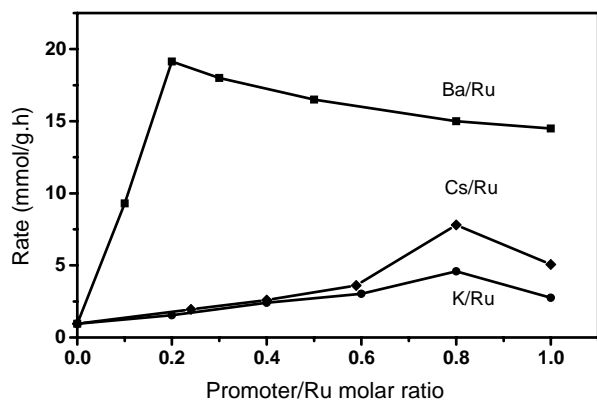
Fig. 4. Ammonia synthesis rates on Ru-Ba/GNFs-B as a function of the promoter/Ru atomic ratio.

promoted by potassium or cesium with a molar ratio of 0.8. Comparing the optimized promoter and Ru mole ratio, that of barium is the least. Ru/GNFs-B without the addition of the barium promoter shows a much lower catalytic activity in ammonia synthesis, while the activity is considerably enhanced when a barium promoter is added to the catalyst. Ru/GNFs-B and barium alone do not possess high activity for ammonia synthesis. Therefore, it is suggested that the performance of Ru/GNFs in ammonia synthesis is attributable to the combined effect of Ru–carbon–barium complexes. This shows that it is likely that the barium promoter improve N_2 activation by transferring electrons to the Ru metal from the support, i.e. the activation energy for N_2 dissociation adsorption on the Ru metal sites is lowered. Davis and co-workers [27] studied ammonia synthesis over zeolite X supported Ru promoted by barium and suggested that the presence of the Ba promoter can create more high activity sites at the interface between the promoter and metal Ru. Recently, Muhler and co-workers [10] and Kowalczyk and co-workers [28] suggested that Ba plays the role of a structural promoter to control the concentration of active sites. In addition, Kowalczyk and co-workers [29] also studied the decomposition of ammonia on Ru promoted by Ba and Cs in detail and found a different effect of Ba and Cs. However, Jacobsen and co-workers [30] investigated the role of the Ba promoter under reaction gases by in situ HRTEM and suggested that Ba is an electronic promoter.

Fig. 4 clearly shows that the maximum activity for ammonia synthesis was reached at a Ba/Ru atomic ratio of 0.2. This ratio is much smaller than the Ba-Ru/AC catalyst used as an ammonia synthesis catalyst mentioned earlier [8]. The catalytic activity for ammonia synthesis on Ru-Ba/GNFs-A and Ru-Ba/GNFs-B is higher by about 30% compared to that on Ru-Ba/AC. It should be noted that there is no obvious difference in metal Ru particle size on the three catalysts. There are two reasons for the higher activity of Ru-Ba/GNFs when a Ru catalyst with a smaller amount of promoter can produce the maximum rate of ammonia synthesis. One reason is the degree of carbon graphitisation and the other may be attributed to the higher purity of the GNFs. Table 1 shows

some results from the analysis of several supports. The specific surfaces of our graphitic-nanofilaments are about 278 and 140 m^2/g by N_2 adsorption at 77 K, which are larger than that used in Ref. [18]. This difference may be due to a different preparation method of the carbon nanofilaments and catalysts used. Elemental analysis shows that activated carbon contains some impurities such as S, N, O and Cl electron acceptors (Table 1), while the two types of GNFs only contain traces of oxygen and hydrogen. It should be noted that oxygen and hydrogen species may be created by a pretreatment process with HNO_3, which is used to remove the residual Co or Ni catalyst and support from the GNFs. These functional groups are assumed to improve the dispersion of the deposited metal. It is suggested that electron-withdrawing impurities, such as S, N, Cl, etc. could have adverse effects on the activation of N_2 on the Ru surface and also consume part of the promoter [5,17]. Therefore, the complete removal of electron-acceptors on activated carbon is an important factor for the catalytic activity of the catalyst. This is one reason for the pretreatment of activated carbon at high temperatures [4,6,7,9].

The catalytic activity slowly decreases with increasing amount of the barium promoter when the Ba/Ru atomic ratio is above 0.3. The decrease in the ammonia synthesis rate with an increase in the Ba/Ru molar ratio is probably due to excessive surface active sites blocked by excess Ba species. Therefore, a reasonable amount of barium should be used to modify the Ru crystalline face to give a more active sites.

The ammonia synthesis rate curve against the increase in Ru content is shown in Fig. 5. It is found that catalytic activation slowly increases with an increase in Ru loading on GNFs, but this is not very apparent and is not in proportion to the Ru content. The size analysis of Ru particles by TEM (Fig. 2) showed a size increase of the Ru particles for 8 wt.% Ru/GNFs-B. This means that the size of the metal particles is an important key in the activity for ammonia synthesis. However, it should be noted that the shape of the Ru particles of 8 wt.% Ru/GNFs-B is not similar to that of
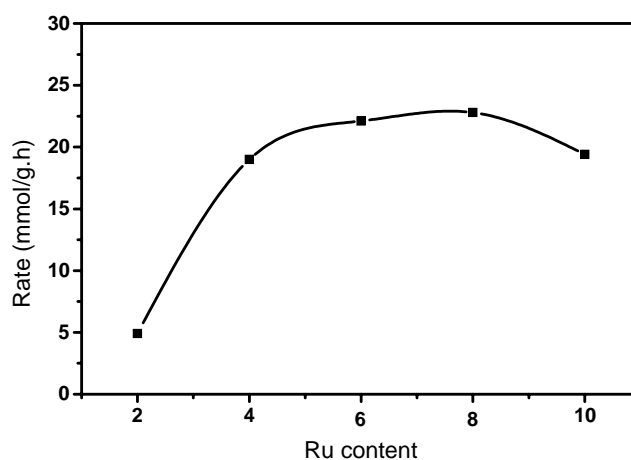

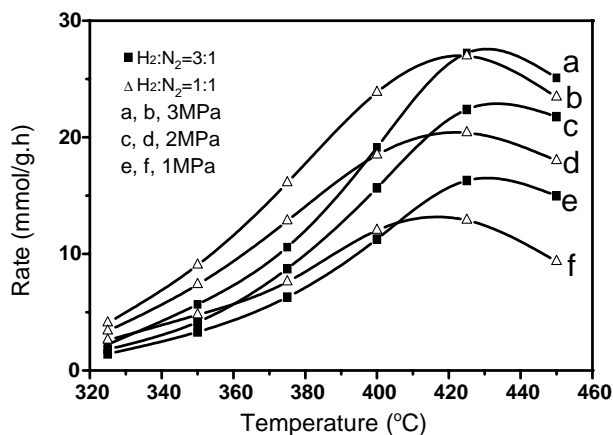Fig. 5. Ammonia synthesis rates on Ru-Ba/GNFs-B as a function of Ru content.

Fig. 6. Pressure and gas composition dependence of the ammonia synthesis activity of 4 wt.% Ru-Ba/GNFs-B catalysts. Measurements were carried out using a gas mixture flow of 50 ml min^{-1} (STP).

Fig. 7. Ammonia synthesis rates on 4 wt.% Ru-Ba/GNTs as a function of time. Measurements were performed using a mixture of $H_2/N_2 = 3$ and a flow of 50 ml min^{-1} (STP) at 450 °C and 3.2 MPa.

4 wt.% Ru/GNFs-B. Therefore, the possible explanation for the relation of Ru content and catalytic activity is that metal Ru particles of about 2–3 nm are most efficient for ammonia synthesis, while more active surface sites could not be supported even when using high content Ru-containing catalyst. In addition, the shape of the metal Ru particles, which can produce a large number of efficient surface sites for ammonia synthesis, is also responsible for the high activity performance of the catalyst for ammonia synthesis. The conversions of a N_2 to H_2 mixture are shown in Fig. 6. It can be seen that the activity increases with an increase in temperature and pressure at a constant H_2/N_2 molar ratio. This indicates that higher pressures and temperatures are favorable for ammonia synthesis. However, the results from different H_2/N_2 molar ratios show that a higher H_2/N_2 molar ratio in the feed gas is not favorable to a higher activity at lower temperatures. This result is in agreement with previous reports [12,27,31], indicating that H_2 is an inhibitor, i.e. the active sites of Ru were covered by adsorbed hydrogen atoms which inhibit N_2 dissociation. However, it was found that H_2 inhibition of N_2 activation at low temperatures is significantly lowered when using a higher P_{N_2}/P_{H_2} molar ratio. Therefore, from an energy saving perspective, a higher N_2 and H_2 atomic ratio is an important advantage of Ru/GNFs catalysts for ammonia synthesis at lower temperatures.

We have also studied the power rate law expression of ammonia synthesis under steady state conditions. This is derived from the ammonia outlet concentration measurements. The determination of the reaction order with respect to N_2 and H_2 is the same as reported in Ref. [21]. It is found that the power law can be expressed as $r = K P_{NH_3}^{-0.4} P_{N_2}^{0.8} P_{H_2}^{-0.7}$, indicating that the effect of H_2 and NH_3 on N_2 activation on the surface is adverse. This result is similar to other studies of ammonia synthesis kinetics on different catalysts [2,3,21]. The apparent activation energy is 83 kJ mol^{-1} at a pressure of 3.0 MPa, which is similar to the result obtained

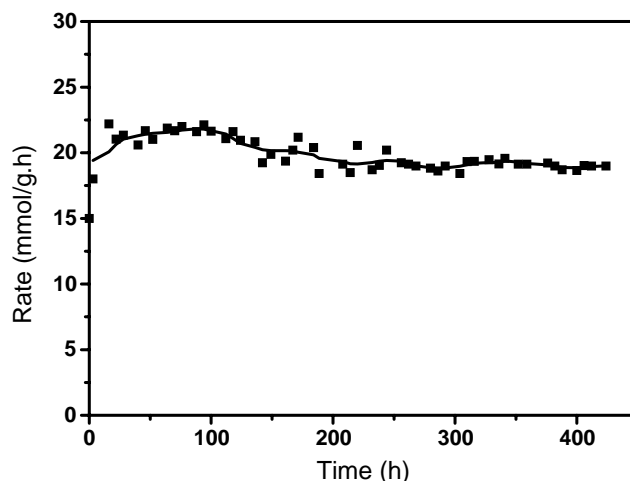on Ru/MgO and Cs$_2$CO$_3$-Ru/MgO and lower than that on CsNO$_3$-Ru/MgO and Ru-Ba/AC catalysts [2,24].

In order to investigate changes in the metal particle and catalytic activity, the 4 wt.% Ru/GNFs-B catalyst was tested for about 420 h at 450 °C and 3.2 MPa using a mixture of $3H_2 + N_2$ with a flow rate 50 ml min^{-1}. Fig. 7 shows the activity change as a function of time. An increase in activity is found at the beginning of the reaction, but then the activity remains fairly constant. During the test reaction, the ammonia concentration in the exit reaches the equilibrium value. No obvious deactivation is observed under those conditions after 400 h. It is interesting to note that metal peaks could not be found by XRD after the catalyst was tested for 400 h.
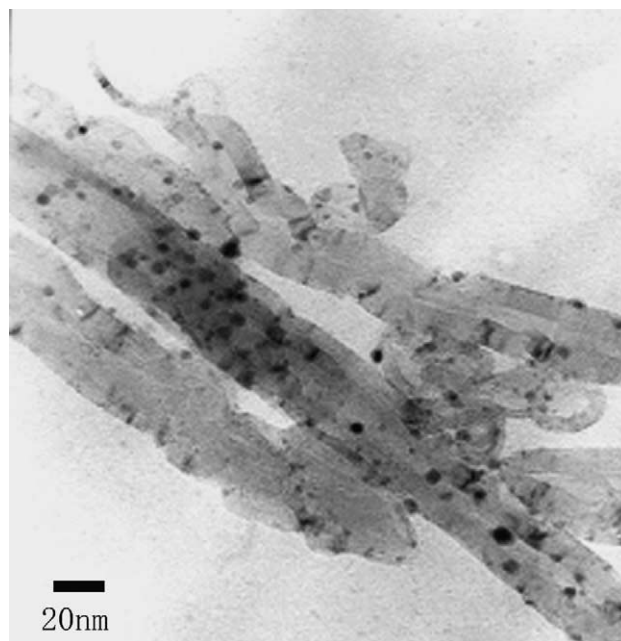

Fig. 8. TEM micrograph of used 4 wt.% Ru/GNFs-B catalyst at 450 °C and 3.2 MPa.

However, larger spherical particle sizes can be observed by TEM and are shown in Fig. 8. As compared to a fresh sample, this may possibly be due to the sintering of smaller metal particles which may accumulate and form efficient crystal facets for ammonia synthesis or the metal particles are covered by the Ba promoter [30]. Ru/MgO for ammonia synthesis was studied by Muhler and co-workers [11] who reported a long induction period is necessary. In addition, N_2 activation on Ru was investigated and B5 type sites are believed to be mainly responsible for N_2 dissociation by van Hardeveld and van Montefoort [32] and Chorkendorff and co-workers [33]. Jacobsen et al. [24] also suggested that the support plays an important role in controlling the morphology of the Ru crystals. Therefore, a shorter induction time for Ru-Ba/GNFs is needed since more active sites of Ru are formed on the graphitic-nanofilaments due to a special interaction between Ru and GNFs.

4. Conclusions

The activity of Ru-Ba/GNFs catalysts is higher by about 25% compared to that of Ru-Ba/AC. TEM shows that Ru metal particles on GNFs have a size ranging from 2 to 4 nm. The temperature for initial methanation of Ru/GNFs is much higher than that of Ru/AC. XRD results show that GNFs have high graphitization compared to activated carbon. A catalyst promoted with Ba is more active than that with K or Cs. The power law can be expressed by $r = KP_{NH_3}^{-0.4} P_{N_2}^{0.8} P_{H_2}^{-0.7}$ and H_2 is an inhibitor of N_2 activation. Single-walled and multi-walled nanofilaments used as the supports show negligible activity difference for ammonia synthesis.

References

[1] A. Ozaki, K. Aika, H. Hori, Bull. Chem. Soc. Jpn. 44 (1971) 3216.
[2] F. Rosowski, A. Hornung, O. Hinrichsen, D. Herein, M. Muhler, G. Ertl, Appl. Catal. A 151 (1997) 443.
[3] S. Hagen, R. Barfod, R. Fehrman, C.J.H. Jacobsen, H.T. Teunissen, K. Ståhl, I. Chorkendorff, Chem. Commun. (2002) 1206.
[4] H.S. Zeng, K. Inazu, K. Aika, Appl. Catal. A 219 (2001) 235.
[5] H.S. Zeng, T. Hihara, K. Inazu, K. Aika, Catal. Lett. 76 (2001) 193.
[6] L. Forni, D. Molinari, I. Rossetti, N. Pernicone, Appl. Catal. A 185 (1999) 269.
[7] Z. Kowalczyk, S. Jodzis, W. Raróg, J. Zielinski, J. Pielaszek, A. Presz, Appl. Catal. A 184 (1999) 95.
[8] C. Liang, Z. Wei, Q. Xin, C. Li, Appl. Catal. A 208 (2001) 193.
[9] Z. Kowalczyk, J. Sentek, S. Jodzis, R. Diduszko, A. Presz, A. Terzyk, Z. Kucharski, J. Suwalski, Carbon 34 (1996) 403.
[10] D. Szmigiel, H. Bielawa, M. Kurtz, O. Hinrichsen, M. Muhler, W. Raróg, S. Jodzis, Z. Kowalcyzk, L. Znak, J. Zieliñski, J. Catal. 205 (2002) 205.
[11] H. Bielawa, O. Hinrichsen, A. Birkner, M. Muhler, Angew. Chem. Int. Ed. 40 (2001) 1061.
[12] O. Hinrichsen, F. Rosowski, A. Hornung, M. Muhler, G. Ertl, J. Catal. 165 (1997) 33.
[13] C.J.H. Jacobsen, J. Catal. 200 (2001) 1.
[14] S. Iijima, Nature 354 (1991) 56.
[15] K.P.D. Jong, J.W. Geus, Catal. Rev. Sci. Eng. 42 (4) (2000) 481.
[16] R. Satio, M. Fujita, G. Dresselhaus, M.S. Dresselhaus, Appl. Phy. Lett. 60 (1992) 2204.
[17] M. Muhler, F. Rosowski, O. Hinrichsen, A. Hornung, G. Ertl, Stud. Surf. Sci. Catal. 101 (1996) 317.
[18] H.B. Chen, J.D. Lin, J. Cai, X.Y. Wang, J. Yi, J. Wang, G. Wei, Y.Z. Lin, D.W. Liao, Appl. Surf. Sci. 180 (2001) 328.
[19] C. Liang, Z. Li, J. Qiu, C. Li, J. Catal. 211 (2002) 278.
[20] Q. Liang, B. Liu, S. Tang, Z. Li, Q. Li, L. Gao, B. Zhang, Z. Yu, Acta Chim. Sinica 58 (2000) 1336.
[21] R. Kojima, K. Aika, Appl. Catal. A 209 (2002) 317.
[22] S. Liu, X. Tang, L. Yin, Y. Koltypin, A. GedanKen, J. Mater. Chem. 10 (2000) 1271.
[23] X. Wang, Y. Liu, D. Zhu, Chem. Phys. Lett. 340 (2001) 419.
[24] C.J.H. Jacobsen, S. Dahl, P.L. Hansen, E. Törnqvist, L. Jensen, H. Topsøe, D.V. Prip, P.B. Møenshaug, I. Chorkendorff, J. Mol. Catal. A: Chem. 163 (2000) 19.
[25] L. Duclaux, Carbon 40 (2002) 1751.
[26] C. Park, R.T.K. Baker, J. Phys. Chem. B 102 (1998) 5168.
[27] B.C. McClaine, T. Becue, C. Lock, R.J. Davis, J. Mol. Catal. A: Chem. 163 (2000) 105.
[28] W. Raróg, Z. Kowalczyk, J. Sentek, D. Skladanowski, J. Zielinski, Catal. Lett. 68 (2000) 163.
[29] W. Raróg, D. Szmigiel, Z. Kowalczyk, S. Jodzis, J. Zielinski, J. Catal. 218 (2003) 465.
[30] T.W. Hansen, J.B. Wagner, P.L. Hansen, S. Dahl, H. Topsøe, C.J.H. Jacobsen, Science 294 (2001) 1508.
[31] S.R. Tenison, in: J.R. Jennings (Ed.), Catalytic Ammonia Synthesis, first ed., Plenum Press, New York, 1991, p. 303.
[32] R. van hardeveld, A. van Montefoort, Surf. Sci. 4 (1996) 396.
[33] S. Dahl, E. Törnqvist, I. Chorkendorff, J. Catal. 192 (2000) 381.